Published as: *Cell*. 2010 August 20; 142(4): 556–567.

The monopolin complex cross-links kinetochore components to regulate chromosome-microtubule attachments

Kevin D. Corbett[1], **Calvin K. Yip**[2], **Ly-Sha Ee**[3], **Thomas Walz**[2,4], **Angelika Amon**[3,4], and **Stephen C. Harrison**[1,4,*]

[1] Department of Biological Chemistry and Molecular Pharmacology, Harvard Medical School, 250 Longwood Avenue, Boston, Massachusetts 02115, USA

[2] Department of Cell Biology, Harvard Medical School, 240 Longwood Avenue, Boston, Massachusetts 02115, USA

[3] David H. Koch Institute for Integrative Cancer Research, Massachusetts Institute of Technology, E17-233, 40 Ames Street, Cambridge MA 02139 USA

[4] Howard Hughes Medical Institute

Summary

The monopolin complex regulates different types of kinetochore-microtubule attachments in fungi, ensuring sister chromatid co-orientation in *S. cerevisiae* meiosis I and inhibiting merotelic attachment in *S. pombe* mitosis. In addition, the monopolin complex maintains the integrity and silencing of ribosomal DNA (rDNA) repeats in the nucleolus. We show here that the *S. cerevisiae* Csm1/Lrs4 monopolin subcomplex has a distinctive V-shaped structure, with two pairs of protein-protein interaction domains positioned ~10 nm apart. Csm1 presents a conserved hydrophobic surface patch that binds two kinetochore proteins: Dsn1, a subunit of the outer-kinetochore MIND/Mis12 complex, and Mif2/CENP-C. Csm1 point-mutations that disrupt kinetochore-subunit binding also disrupt sister chromatid co-orientation in *S. cerevisiae* meiosis I. We further show that the same Csm1 point-mutations affect rDNA silencing, probably by disrupting binding to the rDNA-associated protein Tof2. We propose that Csm1/Lrs4 functions as a molecular clamp, cross-linking kinetochore components to enforce sister chromatid co-orientation in *S. cerevisiae* meiosis I and to suppress merotelic attachment in *S. pombe* mitosis, and cross-linking rDNA repeats to aid rDNA silencing.

Introduction

Mitosis and meiosis are related processes in which duplicated eukaryotic chromosomes segregate to daughter cells or gametes (Lee and Amon, 2001; Marston and Amon, 2004; Nasmyth, 2001). In mitosis, chromosomes replicate and the resulting sister-chromatid pairs are held together along their length by cohesin complexes. Associated with the centromere of each chromatid is a kinetochore, a specialized protein assembly that captures microtubules (MTs) of the mitotic spindle. In early mitosis, each sister chromatid pair becomes ‘bi-oriented’ when its kinetochores capture MTs extending from opposite spindle poles. Once each chromatid pair is properly attached, cleavage of the cohesin links between sisters allows chromosome segregation and subsequent cell division.

*To whom correspondence should be addressed. harrison@crystal.harvard.edu. Phone: (617) 432-5607. Fax: (617) 432-5600.

DNA replication and cell division strictly alternate in mitosis, but in meiosis, DNA replication is followed by two successive divisions to yield four haploid gametes. During meiotic prophase, homologous chromosomes align and form crossovers that hold them together. This organization allows for bi-orientation and segregation of homologs in meiosis I, followed by segregation of sister chromatids in meiosis II (Lee and Amon, 2001; Marston and Amon, 2004; Nasmyth, 2001). Thus, while sister chromatids bi-orient and segregate from each other in mitosis and meiosis II, they instead co-orient and segregate together in meiosis I.

In the budding yeast *Saccharomyces cerevisiae*, sister chromatid co-orientation in meiosis I depends on the four-protein monopolin complex (Mam1, Csm1, Lrs4, and Hrr25/casein kinase 1), which localizes to centromeres from meiotic prophase through metaphase I (Monje-Casas et al., 2007; Petronczki et al., 2006; Rabitsch et al., 2003; Toth et al., 2000). Mam1 is expressed specifically in meiosis (Toth et al., 2000) and associates at centromeres with the ubiquitous kinase Hrr25 (Petronczki et al., 2006). The remaining subunits, Csm1 and Lrs4, form a complex that resides in the nucleolus during interphase and relocalizes to centromeres during meiotic prophase, accompanied by phosphorylation of Lrs4 (Huang et al., 2006; Katis et al., 2004; Lo et al., 2008; Matos et al., 2008; Rabitsch et al., 2003). Robust centromeric localization of Csm1/Lrs4 requires Mam1 (Rabitsch et al., 2003). It has been proposed that the monopolin complex cross-links and/or co-orients sister kinetochores in meiosis I, so that they attach to microtubules (MTs) extending from the same spindle pole (Monje-Casas et al., 2007). Although monopolin complex subunits have not been identified outside of fungi, the concept of sister kinetochore 'fusion' in meiosis I may have parallels in higher eukaryotes: in maize meiosis I, for example, inner kinetochores of sister chromatids can be resolved by fluorescence microscopy, while their outer kinetochores appear fused (Li and Dawe, 2009).

Orthologs of the monopolin subunits Csm1 and Lrs4 are present in the fission yeast *Schizosaccharomyces pombe* (Pcs1 and Mde4, respectively) and also cycle between the nucleolus and kinetochores (Gregan et al., 2007; Rabitsch et al., 2003). These proteins inhibit merotelic attachment (capture of a single kinetochore by MTs from opposite spindle poles) during mitosis, but they do not contribute to sister chromatid co-orientation in meiosis I. (An unrelated protein, Moa1, is important for ensuring meiosis I sister co-orientation in *S. pombe*, probably by modifying cohesin-complex function near centromeres (Yokobayashi and Watanabe, 2005)). While *S. cerevisiae* kinetochores capture a single MT, *S. pombe* and higher eukaryotes assemble larger kinetochores that capture multiple MTs (2-4 in *S. pombe* (Ding et al., 1993), 15-30 in metazoans (McEwen et al., 1997)). In this context, Pcs1 and Mde4 have been proposed to organize *S. pombe* kinetochores by clamping together adjacent MT-binding sites (Gregan et al., 2007). In addition, Pcs1 and Mde4 have recently been shown to localize to the mitotic spindle in anaphase, revealing another potential function for monopolin in anaphase spindle elongation and stability (Choi et al., 2009).

During interphase, *S. cerevisiae* Csm1/Lrs4 and *S. pombe* Pcs1/Mde4 are both in the nucleolus, where they have been shown in *S. cerevisiae* to be important for maintaining the ribosomal DNA (rDNA) (Gregan et al., 2007; Huang et al., 2006; Mekhail et al., 2008). The repetitive rDNA array (100-200 copies of a 9.1-kb repeat in *S. cerevisiae*) is normally kept in a silenced, heterochromatin-like state by a network of rDNA-associated proteins, including Fob1, Tof2, Csm1/Lrs4, and the RENT complex (Regulator of nucleolar silencing and telophase exit), which contains Net1/Cfi1, Cdc14, and the Sir2 histone deacetylase (Huang et al., 2006; Huang and Moazed, 2003). The rDNA is also protected from unequal sister chromatid exchange (USCE), which can lead to addition or deletion of repeats within the rDNA (Sinclair and Guarente, 1997). USCE is suppressed by Csm1/Lrs4 (Huang et al., 2006), the inner-nuclear membrane proteins Heh1 and Nur1 (Mekhail et al., 2008), and the condensin complex (Johzuka and Horiuchi, 2009), in addition to Sir2 (Huang et al., 2006; Smith and Boeke, 1997; Smith et al., 1999). With the exception of Sir2, which independently contributes to USCE suppression,

these proteins appear to tether rDNA repeats to the nuclear periphery, sequestering them from recombination factors (Mekhail et al., 2008), and they may also clamp sister chromatids together in register (Brito et al., 2010; Johzuka and Horiuchi, 2009). Thus, while Csm1/Lrs4 contributes to both rDNA silencing and USCE suppression, it acts with distinct sets of proteins in these different processes, raising the question of whether a common mechanism underlies these activities.

The regulatory functions of monopolin described above suggest that Csm1/Lrs4 and the orthologous Pcs1/Mde4 are molecular cross-linkers, joining MT-binding elements at kinetochores and rDNA repeats in the nucleolus. We report here that *S. cerevisiae* Csm1 and Lrs4 form a complex with a distinctive 'V' shape, which positions two pairs of protein-protein interaction domains ~10 nm apart. We find that a conserved surface patch on these domains binds two kinetochore subunits: Dsn1, a subunit of the outer-kinetochore MIND/Mis12 complex, and Mif2/CENP-C. Point-mutations in this conserved surface disrupt both Dsn1 and Mif2 binding *in vitro* and cause bi-orientation of sister chromatids in meiosis I. These data are consistent with a model of monopolin as a cross-linker that clamps kinetochores together to enforce co-orientation in *S. cerevisiae* meiosis I and inhibit merotelic attachment in *S. pombe* mitosis. We also find that Csm1 interacts with the nucleolar protein Tof2 through the same conserved surface that interacts with Dsn1 and Mif2, and that mutating the Csm1 surface patch also disrupts rDNA silencing. These mutations do not, however, affect the rate of unequal sister chromatid exchange, demonstrating that Csm1/Lrs4 has two biochemically separate roles in the maintenance of rDNA. Overall, our data show that Csm1/Lrs4 is a molecular cross-linker that regulates kinetochore-microtubule attachment and helps preserve rDNA integrity.

Results

Structure of Csm1

We purified full-length *S. cerevisiae* Csm1 and *S. pombe* Pcs1 proteins, as well as truncations lacking the bulk of their N-terminal regions, which are predicted to form coiled-coils (Gregan et al., 2007; Rabitsch et al., 2003). By sedimentation equilibrium analytical ultracentrifugation, we found that both constructs of Csm1 and Pcs1 are homodimers in solution (Table 1). We obtained crystals of both full-length *S. cerevisiae* Csm1 and the isolated C-terminal domain (residues 69-181 of 190). We determined the structure of the C-terminal domain to 2.35 Å resolution using anomalous diffraction methods with selenomethionine-derivatized protein (see Table S1 for crystallographic statistics), and we then determined the structure of the full-length protein to 3.4 Å resolution by molecular replacement. The structures show that Csm1 has a 12-nm long, N-terminal coiled-coil (residues 3-82), and a C-terminal globular domain (residues 83-181) containing three α-helices and five β-strands (Figure 1A). The β-sheet of each monomer wraps around the N-terminal α-helix of its dimer mate, forming an intimate dimer interface.

Csm1 is a structural relative of the kinetochore proteins Spc24 and Spc25 (Figure 1B,C) (Wei et al., 2006). These proteins are paralogs that form a heterodimer similar to the Csm1 homodimer and constitute the inner half of the conserved Ndc80 kinetochore complex (Joglekar et al., 2006; Wei et al., 2005). The similarity of the tertiary and quaternary structures of Csm1 and Spc24/Spc25 imply a common evolutionary origin, despite their very low sequence identity (<15%). The C-terminal globular domains of Spc24 and Spc25 are thought to connect the Ndc80 complex with proteins of the inner kinetochore, suggesting that this domain of Csm1 may also be a protein interaction module. Inspection of amino acid conservation among 41 fungal Csm1/Pcs1 orthologs reveals a conserved surface patch on the face directly opposite the coiled-coil, bordering α-3, β-5, and α-4 (Figure 1D, Figure S1). The patch faces away from the dimer interface, so that the Csm1 dimer has two conserved surfaces centered ~3 nm from each other. As both α-3 and β-5 are located in a Csm1-specific insertion

in the globular domain, this surface is not present in Spc24/Spc25. Therefore, it is unlikely that Csm1 and Spc24/Spc25 have a common binding site at kinetochores, despite their overall structural similarity.

Structure of the Csm1/Lrs4 complex

S. cerevisiae Csm1 and Lrs4 are known to interact through their N-terminal coiled-coil regions (Rabitsch et al., 2003). Co-expression of Csm1 with full-length Lrs4 (347 residues) or with an isolated N-terminal segment (residues 1-130 or 1-102) yields a complex with four copies of Csm1 and two copies of Lrs4 (Table 1). Co-expression of *S. pombe* Pcs1 and Mde4 also yields a complex with 4:2 stoichiometry, with the N-terminal region of Mde4 (residues 1-77 of 421 is the smallest segment we have tested) sufficient for complex formation (Table 1, Figure S2).

We obtained crystals of the complex between *S. cerevisiae* Csm1 and residues 1-102 of Lrs4, which diffracted anisotropically to between 6.0 Å (along the a* and b* reciprocal unit-cell axes) and 3.9 Å (along c*) resolution, and we determined the structure by molecular replacement. We located two Csm1 homodimers per asymmetric unit and found that the N-terminal coiled-coils of these two dimers sandwich two closely-packed, parallel, 30-amino acid α-helices, creating a 'V'-shaped complex that positions the two pairs of Csm1 globular domains ~10 nm apart (Figure 2A,B).

Our electron density maps indicated that two copies of a ~30-amino acid region of Lrs4 might be sufficient for complex formation with Csm1, but the low resolution precluded direct assignment of sequence to this electron density. From sequence conservation and secondary structure predictions, it appeared that the density probably represented two N-terminal segments of Lrs4, with the remainder of the protein (approximately residues 34-102) disordered in our crystals. Mixing Csm1 with a peptide containing Lrs4 residues 2-30 results in a stable complex with the expected molecular mass for a 4:2 complex (Table 1, Figure S2). This complex also forms crystals isomorphous to those of the complex with Lrs4 1-102 (data not shown), supporting the inference that Lrs4 residues 34-102 are disordered in the latter crystals and hence do not contribute to the diffraction intensities. We established the orientation and sequence register of the Lrs4 α-helices using selenomethionine anomalous scattering from a construct containing a L8→M mutation in Lrs4. We observed a single anomalous difference peak in the electron density maps, directly between the two Lrs4 α-helices (Figure 2C); at this resolution (6.0/3.9 Å), the single peak probably represents the anomalous scattering of both Se atoms in the Lrs4 dimer. This assignment indicates that the disordered C-terminal region of Lrs4 extends outward from the base of the observed 'V'.

We also examined the architecture of the native Csm1/Lrs4 complex using negative-stain electron microscopy. We purified Csm1/Lrs4 from mitotically cycling *S. cerevisiae* by TAP-tagging Lrs4, thus obtaining a near-native nucleolar form of Csm1/Lrs4. Individual particles of this complex, as well as of the recombinant Csm1/Lrs4 1-102 complex, show a clear V shape (Figure 2D,E), and class averages of the native full-length complex can be matched with 2-D projections of the x-ray structure (Figure 2F). We can draw two conclusions from the close correspondence of the projections and class averages. First, the conformation of the complex is stiff and not grossly affected by the packing in our crystals. Second, the bulk of the two Lrs4 subunits is either largely disordered in solution or flexibly linked to the rest of the complex. This conclusion is consistent with our observation that residues ~34-102 were disordered in the crystal structure of Csm1/Lrs4 1-102. The C-terminal region of Lrs4 is nonetheless crucial for regulation of monopolin: phosphorylation and dephosphorylation of Lrs4 (and its *S. pombe* ortholog Mde4) is needed for localization and activity at kinetochores (Choi et al., 2009; Katis et al., 2004; Lo et al., 2008; Matos et al., 2008), and even a small C-terminal deletion of Lrs4 (23 residues) compromises function in the nucleolus (Johzuka and Horiuchi, 2009).

Csm1 binds two kinetochore subunits

Previous attempts to identify direct binding partners of Csm1/Lrs4 using TAP-tagging and mass spectrometry have not identified any kinetochore subunits, which are present in relatively low abundance in the cell (Huang et al., 2006; Petronczki et al., 2006). The kinetochore proteins Ctf19 and Dsn1 were recently identified as potential Csm1 binding partners by a large-scale two-hybrid screen focused on *S. cerevisiae* kinetochore proteins (Wong et al., 2007). Ctf19 is part of the COMA complex, which is not well-conserved in higher eukaryotes, while Dsn1 is a component of the highly conserved MIND/Mis12 complex (Cheeseman and Desai, 2008). In addition, a recent study identified an interaction between *S. pombe* Pcs1 and the inner-kinetochore protein Cnp3/CENP-C (*S. cerevisiae* Mif2), also by yeast two-hybrid analysis (Tanaka et al., 2009). We tested binding of *in-vitro* translated and [35]S-labeled Dsn1, Ctf19, and Mif2 to several constructs of Csm1, using a Ni2+-affinity pulldown assay. While Ctf19 did not bind Csm1 (data not shown), both Dsn1 and Mif2 bound to full-length Csm1 and to the isolated C-terminal globular domain, but not to the isolated N-terminal coiled-coil region (Figure 3 A). As Csm1 has previously been shown to interact with the monopolin subunit Mam1 (Rabitsch et al., 2003), we also tested binding of this protein to our Csm1 constructs and found that Mam1 binds specifically to the C-terminal globular domain of Csm1 (Figure 3A). We next tested whether Dsn1, Mif2, or Mam1 binding was affected by point mutations in the conserved hydrophobic surface patch on the Csm1 globular domain. None of the mutations tested affected Mam1 binding (Figure 3A), but three of them, Y156→E, L161→D, and L161→K, substantially reduced binding of both Dsn1 and Mif2 (Figure 3A). These results indicate that both Dsn1 and Mif2 contact the conserved surface patch on Csm1 and may even compete for a common binding surface, while Mam1 probably binds elsewhere on the Csm1 C-terminal domain.

To confirm and extend these results, we purified the four-protein MIND (Mtw1 including Nsl1, Nnf1, and Dsn1) kinetochore complex (De Wulf et al., 2003), which forms an extended ~25 nm long structure containing one copy of each subunit (Table S2, Figure S3). In the Ni^{2+}-affinity pulldown assay, this purified complex bound full-length Csm1 and the isolated C-terminal globular domain, and mutating Csm1 residues Y156 and L161 disrupted the interaction (Figure S3). Using size exclusion chromatography, we observed that the Csm1/Lrs4 complex co-migrated with purified MIND complex, although some dissociation occurred during the course of the experiment (Figure 3B,C). When the two complexes were present in a 1:4 ratio (Csm1/Lrs4:MIND), essentially all of the Csm1/Lrs4 co-migrated with MIND. When the complexes were present at 1:2 or 1:1 ratios, some Csm1/Lrs4 did not co-migrate with MIND. Thus, each Csm1/Lrs4 complex can probably interact with up to four MIND complexes, meaning that each conserved surface patch in the complex can independently interact with a partner protein (Figure 3C).

As the conserved Csm1 surface patch is shared in all fungal Csm1/Pcs1 orthologs (Figure S1), Dsn1 and/or Mif2 may represent conserved binding partners for these proteins. To test this idea, we performed Ni^{2+}-affinity pulldown assays using *S. pombe* Pcs1 as bait, and the *S. pombe* Dsn1 and Mif2 orthologs, Mis13 and Cnp3, as prey. We found that the *S. pombe* Pcs1 C-terminal domain interacts with Mis13, and with both full-length Cnp3 and the minimal Pcs1-binding fragment identified previously, amino acids 130-270 (Figure 3D) (Tanaka et al., 2009). Binding to both Mis13 and Cnp3 was disrupted by mutations to Pcs1 residues Y197 and I202 (Figure 3D), which correspond to *S. cerevisiae* Csm1 residues Y156 and L161, respectively (Figure S1). Thus, *S. cerevisiae* Csm1 and *S. pombe* Pcs1 bind orthologous kinetochore subunits through the conserved surface patch on their C-terminal globular domains.

Csm1 point mutations disrupt sister chromatid co-orientation in meiosis I

Deletion of any single monopolin subunit in *S. cerevisiae* results in mis-segregation of chromosomes in meiosis I (Petronczki et al., 2006; Rabitsch et al., 2003; Toth et al., 2000). In order to observe sister chromatid MT attachment geometry in meiosis I, we used an *S. cerevisiae* strain bearing an array of TET operator sequences inserted at the chromosome V centromere and also expressing a fusion of GFP and the Tet repressor protein, which binds to the operator sites (referred to as *CENV*-GFP) (Lee and Amon, 2003). We introduced *CSM1* point-mutations into a strain heterozygous for *CENV*-GFP and with the endogenous promoter of *CDC20* replaced by that of *CLB2*, to arrest the cells in metaphase I (Lee and Amon, 2003). The heterozygous *CENV*-GFP marker allows a simple readout of sister chromatid attachment geometry: when the monopolin complex is functioning properly to co-orient sister kinetochores, the GFP signals from the two marked sister centromeres should overlap. If the monopolin complex is compromised, sister kinetochores become bi-oriented, and spindle forces pull the marked sister centromeres far enough apart to form two resolved foci (Lee and Amon, 2003; Monje-Casas et al., 2007; Toth et al., 2000). We introduced the three Csm1 point mutations that disrupt Dsn1/Mif2 binding *in vitro*: Y156→E, L161→D, and L161→K. Two of these, L161→D and L161→K, result in 45% and 41% GFP dot separation, respectively, matching the severity of a *MAM1* deletion (40% separation, see Figure 4A). The third mutation, Y156→E, does not cause elevated levels of sister chromatid bi-orientation *in vivo*, suggesting that the Y156→E mutant retains some affinity for its binding partners at the kinetochore that is not detected by our pulldown assay.

We next used strains carrying *CENV*-GFP on both homologs and the wild-type *CDC20* promoter (no metaphase I arrest) to examine chromosome segregation fidelity through a complete meiosis, by counting GFP signals in the spores of tetrads. In 95% of wild-type tetrads, all four spores contained GFP foci, indicating that each spore had received a single copy of chromosome V (5% faulty segregation; Figure 4B and Table S3). In contrast, a *CSM1* deletion resulted in nearly 80% of tetrads with GFP dots in only three, two or one spore, in close agreement with previous studies (Rabitsch et al., 2003). The three *CSM1* point-mutations all showed statistically significant increases in faulty segregation over wild-type, but varied in severity, with the Y156→E mutation having the mildest effect (16.5% faulty segregation) and L161→D the strongest (58% faulty segregation; Figure 4B). We found a similar range in the effects of the point mutations on spore viability: 88% of spores were viable in the Y156→E mutant, 34% in L161→K, and only 12% in L161→D (wild-type = 93% viable, Δ*csm1* = 4% viable; Figure 4B and Table S3). This range of phenotypes indicates that each point mutation affects Csm1-kinetochore interactions to a different degree, and that none of the mutations completely eliminates kinetochore binding. Overall, however, our results show that mutations to the conserved surface patch of Csm1 cause significant errors in meiotic chromosome segregation, most likely by disrupting Csm1-kinetochore interactions in metaphase I.

Csm1 point mutations affect rDNA silencing

In addition to acting at kinetochores, Csm1 and Lrs4 localize to the nucleolus during interphase, where they participate in rDNA silencing and the suppression of unequal sister chromatid exchange (USCE) (Huang et al., 2006; Huang and Moazed, 2003). Our structure of the Csm1/Lrs4 complex and our studies of its interactions with kinetochore components suggest that it may also cross-link proteins associated with rDNA, potentially through interactions in the conserved surface patch of Csm1. We therefore studied the effects of Csm1 conserved-patch mutations in two assays, one measuring reporter gene silencing and another measuring USCE. To measure rDNA silencing, we compared the growth of yeast strains with an *mURA3* reporter gene inserted at either the *leu2* locus (which is not silenced) or at two locations in the non-transcribed regions of the rDNA repeat (NTS1 or NTS2, Figure 5A), on either complete media or media lacking uracil. This assay has previously shown that the Sir2 histone deacetylase is

required for silencing throughout the rDNA, while a network of proteins associated with the replication-fork block sequence (RFB in Figure 5A), including Fob1 and Tof2 as well as Csm1/Lrs4, are required for silencing specifically in the NTS1 region (Huang et al., 2006; Huang and Moazed, 2003). We found that mutations to the conserved surface patch of Csm1 had the same effect as a *CSM1* deletion: silencing was completely lost at NTS1, and partially lost at NTS2 (Figure 5B).

We next tested the rate of recombination resulting in USCE, which is strongly inhibited in wild-type cells through multiple mechanisms: a Sir2-mediated mechanism presumably dependent on the assembly of silenced chromatin, and tethering of rDNA repeats to the nuclear periphery mediated by Csm1/Lrs4, the inner nuclear membrane proteins Heh1 and Nur1, and possibly condensins (Huang et al., 2006; Huang and Moazed, 2003; Johzuka and Horiuchi, 2009; Kaeberlein et al., 1999; Mekhail et al., 2008). We measured the rate of loss of an *ADE2* reporter gene embedded within the rDNA array and found a greater than three-fold increase in *USCE* when either *CSM1* or *LRS4* was deleted (Figure 5C, Table S4), in agreement with previous results (Huang et al., 2006). In contrast, we found that none of the *CSM1* point-mutations significantly increased USCE (Figure 5C).

These results indicate that the Csm1/Lrs4 complex may have multiple, biochemically distinct roles in rDNA regulation. The behavior of the Csm1 point mutants resembles that of a deletion of *TOF2*, another member of the RFB-bound protein network. A *TOF2* deletion results in loss of rDNA silencing at NTS1, but has much more modest effects on USCE than deletions of *CSM1*, *LRS4*, or *SIR2* ((Huang et al., 2006) and Figure 5C). As previous biochemical purifications of rDNA-associated protein complexes (Huang et al., 2006) and two-hybrid screens (Wong et al., 2007; Wysocka et al., 2004; Yu et al., 2008) had identified Tof2 as a potential binding partner of Csm1, we tested this interaction *in vitro* using Ni^{2+}-affinity pulldowns. We found that full-length Tof2 specifically interacts with the Csm1 C-terminal domain, and that this binding is modestly affected by mutations to the conserved surface patch (Figure 5D). As full-length Tof2 may be poorly behaved in solution, we also looked for truncations of Tof2 that bind Csm1. We identified a region (residues 251-500) that interacts strongly with wild-type Csm1, and binding of which is disrupted by mutations to conserved-patch residues Y156, L161, and K174 (Figure 5D). The effect of the Csm1 K174→E mutation on Tof2 binding is much more pronounced than its effect on binding of either Dsn1 or Mif2 (Figure 3 A). This result, along with the finding that the Y156→E mutation strongly affects Csm1/Lrs4 function at rDNA but has more modest effects at kinetochores, suggests that while Csm1 binds its multiple partners through a common surface, the details of each interaction probably differ.

The finding that Csm1 binds Tof2 through its conserved surface patch, together with the parallels between the behavior of the *TOF2* deletion and the *CSM1* point mutations in genetic assays, indicates that Csm1/Lrs4 and Tof2 probably function together to aid rDNA silencing. This idea fits with the observation that Csm1/Lrs4 depends on Tof2 for specific association with the NTS1 region of rDNA repeats, as measured by chromatin immunoprecipitation (Huang et al., 2006). Nonetheless, the lack of effect on USCE in the *CSM1* point-mutant strains indicates that there is probably a Tof2-independent function for Csm1/Lrs4 in suppressing rDNA recombination. To determine if Csm1/Lrs4 nucleolar localization is maintained upon disruption of the Csm1-Tof2 interaction, we examined Lrs4 localization during interphase in strains with either a deletion of *TOF2* or with *CSM1* point mutations (Y156→E or L161→D). Wild-type cells showed a pattern of Lrs4 staining characteristic of nucleolar localization (Figure 5E). In contrast, the *TOF2* deletion and *CSM1* point-mutant strains showed mislocalization of Lrs4, with the protein found dispersed throughout the nucleus (Figure 5E). In the *TOF2* deletion strain, but not the *CSM1* point-mutant strains, some cells showed visible enrichment of Lrs4 in a nuclear region that stained poorly with DAPI, suggesting that Csm1/

Lrs4 may still be partially localized to the nucleolus in the absence of interactions with Tof2. The more complete dispersal of Lrs4 in the *CSM1* point-mutant strains as compared to the *TOF2* deletion also suggests that the Csm1 conserved surface patch may mediate interactions with multiple partners in the nucleolus, as it does at kinetochores.

Discussion

The eukaryotic kinetochore is a large multi-protein structure that creates a dynamic connection between chromosomes and MTs. The most likely candidate for direct MT binding in the outer kinetochore is the ~57 nm-long Ndc80 complex (Ciferri et al., 2008; Wei et al., 2007), of which there are 6-8 copies in each *S. cerevisiae* kinetochore (Joglekar et al., 2006). These complexes cooperate to bind a single MT and extend outward from a 'linker' layer of protein complexes, including the MIND/Mis12 complex, which in turn bind inner kinetochore components, including the specialized CENP-A histone and the DNA-binding Mif2/CENP-C protein (Cheeseman et al., 2006; Joglekar et al., 2006; Wei et al., 2007; Wei et al., 2005). A single MT is 25 nm wide, and the V-shaped Csm1/Lrs4 complex presents two pairs of kinetochore-binding globular domains separated by ~10 nm. A plausible model for the mechanism of sister chromatid co-orientation by monopolin, then, is that these two pairs of globular domains bind across sister kinetochores, bringing them so close together that they effectively fuse and create a single, composite MT-binding site (Figure 6A,B). This picture of kinetochore fusion is consistent with measures of spindle MT numbers indicating that, in meiosis I, each pair of sister kinetochores probably attaches to only a single MT (Winey et al., 2005). We cannot currently speculate about the exact geometry of sister kinetochore fusion: each Csm1/Lrs4 complex can probably bind four partners, and each of its kinetochore binding partners is present in multiple copies at each kinetochore (two copies of Mif2, ~6 copies of Dsn1) (Joglekar et al., 2006). Thus, the interactions between Csm1/Lrs4 and kinetochores are likely to be complex and stochastic, resulting in promiscuous cross-linking of nearby elements both within individual kinetochores and between sister kinetochores. Moreover, the relative importance of Csm1 interactions with its two thus-far kinetochore binding partners, Dsn1 and Mif2, remains uncertain. Finally, it is also unknown how Mam1, which binds the Csm1 globular domain and is required for robust Csm1/Lrs4 localization to kinetochores (Rabitsch et al., 2003), might regulate or strengthen specific interactions between Csm1 and its binding partners at the kinetochore.

S. pombe Pcs1 has overall sequence similarity to *S. cerevisiae* Csm1, with high conservation in the kinetochore-binding surface patch. We have shown that the Pcs1/Mde4 complex has the same general architecture as *S. cerevisiae* Csm1/Lrs4 and that it interacts with orthologous binding partners (Dsn1/Mis13 and Mif2/Cnp3). From this evidence, we envision a cross-linking mechanism for monopolin in *S. pombe* that is conceptually similar to its mechanism in *S. cerevisiae*, but functioning within a single kinetochore rather than across sister chromatids. The kinetochores of *S. pombe* are larger than those of *S. cerevisiae*, and they attach to 2-4 MTs through about 20 Ndc80 complexes (Ding et al., 1993; Joglekar et al., 2008). In this context, monopolin-mediated cross-linking of inner kinetochore elements could organize the outer kinetochore and force co-orientation of adjacent MT-binding sites.

Our structural and functional data also help clarify the functions of Csm1/Lrs4 in maintaining the integrity of rDNA. Together with previous data (Huang et al., 2006), our results indicate that the Csm1/Lrs4 complex is recruited to the NTS1 region of rDNA repeats through a direct interaction with Tof2, and that this interaction is important for rDNA silencing. As a deletion of Tof2 does not significantly affect association of Sir2 with the rDNA (Huang et al., 2006), the loss of rDNA silencing in our mutants cannot be due to simple loss of Sir2 localization. We propose that Csm1/Lrs4 cross-links multiple rDNA repeats (up to four per Csm1/Lrs4 complex) through interactions with rDNA-associated Tof2, thereby assisting localized Sir2 in

silencing these now closely juxtaposed/clustered repeats (Figure 6C). This rDNA repeat clustering/cross-linking by Csm1/Lrs4 and Tof2 must not, however, directly suppress unequal sister chromatid exchange, as disrupting the Csm1-Tof2 interaction does not affect the rate of USCE. We propose that, instead, Csm1/Lrs4 may control recombination through interactions with a different set of proteins: the inner nuclear membrane proteins Heh1 and Nur1 (Mekhail et al., 2008) and condensin complexes (Johzuka and Horiuchi, 2009). These interactions mediate the tethering of rDNA repeats to the nuclear periphery and may also link sister chromatids together in-register to suppress unequal exchange (Figure 6D). There is probably some functional interplay between these distinct protein networks controlling rDNA silencing and unequal sister chromatid exchange. The structures and interactions we have described now provide a basis for determining how Csm1/Lrs4 contributes to the activities of each of these protein networks and to their interactions at rDNA.

Experimental Procedures

(For detailed methods, see Extended Experimental Procedures)

Protein expression and purification

All proteins were expressed in *E. coli* with TEV-protease cleavable His_6 tags, and purified by Ni^{2+}, ion-exchange, and gel filtration chromatography. For sedimentation equilibrium analytical ultracentrifugation, proteins were spun in a Beckman Optima XL-A centrifuge at three speeds, which varied with the expected molecular weight of the protein/complex.

Crystallization and structure determination

Protein crystallization is described in the Extended Experimental Procedures. All datasets were collected on NE-CAT beamlines 24ID-C and 24ID-E at the Advanced Photon Source at Argonne National Laboratory. The structure of Csm1 69-181 was determined by single-wavelength anomalous dispersion (SAD) in space group R3 at 2.6 Å resolution, from a selenomethione-labeled crystal of Csm1 69-181 (L157M), then determined by molecular replacement in space group $P2_12_12$ at 2.35 Å resolution. The structure of full-length Csm1 was determined by molecular replacement in space group $P3_121$ to 3.4 Å resolution. The Csm1 1-181/Lrs4 1-102(Δ38-44) complex structure was determined by molecular replacement. Because of the low resolution (6.0/3.9 Å) of the data, refinement was limited to rigid-body and restrained B-factor refinement (see Table S1 for data and refinement statistics).

Electron microscopy

Native Csm1/Lrs4 was purified as described (Huang et al., 2006), adsorbed to glow-discharged carbon-coated copper grids, and stained with 0.75% (w/v) uranyl formate (Ohi et al., 2004). Images were collected with a Tecnai T12 electron microscope (FEI, Hillsboro, OR) operated at 120 kV using low-dose procedures, and processed using SPIDER software (Frank et al., 1996).

Ni^{2+} affinity pulldown assay

Bait proteins were purified as described above with His_6-tags left intact, and $^{[35]}$S-labeled prey proteins were produced using an *in vitro* coupled transcription/translation kit (Promega). Pull-down assays were performed essentially as described (Rabitsch et al., 2003).

Yeast Strains, sporulation, and immunofluorescence

Strains were generated with PCR-based methods as described (Longtine et al., 1998). For spore viability, cells were grown on YPD agar, then patched onto SPO medium (1% KOAc) for 48-72 hours. Forty tetrads (160 spores) were dissected for each strain. For metaphase I bi-orientation,

cells were grown in YPD, then diluted into BYTA (YEP + 1% KOAc/50 mM potassium phthalate) at OD_{600} = 0.3, grown overnight, then washed and resuspended in SPO medium (0.3% KOAc [pH 7.0]) at OD_{600} = 2.0 at 30° C to induce sporulation. Samples were removed hourly for 10 hours, fixed, and stained with DAPI (bi-orientation was assayed at seven hours); arrested cells were scored for one (indicating co-orientation) or two (indicating bi-orientation) *CENV*-GFP foci per nucleus. For *CENV*-GFP segregation to spores, cells were patched onto SPO medium for 48-72 hours, then fixed and stained with DAPI. Tetrads were assayed for GFP foci in DAPI masses. Samples were compared to wild-type using an independent two-sample *t*-test. Indirect immunofluorescence and chromosome spreads were performed as described previously (Visintin et al., 1999).

rDNA Assays

rDNA silencing and unequal sister chromatid exchange assays were performed essentially as described (Huang et al., 2006; Huang and Moazed, 2003; Kaeberlein et al., 1999).

Supplementary Material

Refer to Web version on PubMed Central for supplementary material.

Acknowledgments

We thank the staff at the Advanced Photon Source NE-CAT beamlines for advice and assistance with data collection and interpretation, D. Moazed for the gift of *S. cerevisiae* strains and valuable advice, M. Sawaya for providing advice and script files for anisotropic scaling, J. Al-Bassam for assistance with electron microscopy, members of the Amon laboratory, especially I. Brito and E. Unal, for advice, assistance with yeast strain construction, and light microscopy, and members of the Harrison laboratory and I. Cheeseman for helpful discussions. K.D.C. acknowledges a post-doctoral fellowship from the Helen Hay Whitney Foundation; C.K.Y. acknowledges a post-doctoral fellowship from the Jane Coffin Childs Memorial Fund for Medical Research; T.W., A.A, and S.C.H. are Investigators in the Howard Hughes Medical Institute. Coordinates and structure factors for the reported crystal structures have been deposited with the Protein Data Bank under accession codes 3N4R (Csm1 69-181, R3 form), 3N4S (Csm1 69-181, $P2_12_12$ form), 3N4X (Csm1 full-length), and 3N7N (Csm1/Lrs4 1-102).

References

Brito IL, Yu HG, Amon A. Condensins Promote Co-orientation of Sister Chromatids During Meiosis I in Budding Yeast. Genetics. 2010

Cheeseman IM, Chappie JS, Wilson-Kubalek EM, Desai A. The conserved KMN network constitutes the core microtubule-binding site of the kinetochore. Cell 2006;127:983–997. [PubMed: 17129783]

Cheeseman IM, Desai A. Molecular architecture of the kinetochore-microtubule interface. Nat Rev Mol Cell Biol 2008;9:33–46. [PubMed: 18097444]

Choi SH, Peli-Gulli MP, McLeod I, Sarkeshik A, Yates JR 3rd, Simanis V, McCollum D. Phosphorylation state defines discrete roles for monopolin in chromosome attachment and spindle elongation. Curr Biol 2009;19:985–995. [PubMed: 19523829]

Ciferri C, Pasqualato S, Screpanti E, Varetti G, Santaguida S, Dos Reis G, Maiolica A, Polka J, De Luca JG, De Wulf P, et al. Implications for kinetochore-microtubule attachment from the structure of an engineered Ndc80 complex. Cell 2008;133:427–439. [PubMed: 18455984]

De Wulf P, McAinsh AD, Sorger PK. Hierarchical assembly of the budding yeast kinetochore from multiple subcomplexes. Genes Dev 2003;17:2902–2921. [PubMed: 14633972]

Ding R, McDonald KL, McIntosh JR. Three-dimensional reconstruction and analysis of mitotic spindles from the yeast, Schizosaccharomyces pombe. J Cell Biol 1993;120:141–151. [PubMed: 8416984]

Frank J, Radermacher M, Penczek P, Zhu J, Li Y, Ladjadj M, Leith A. SPIDER and WEB: processing and visualization of images in 3D electron microscopy and related fields. J Struct Biol 1996;116:190–199. [PubMed: 8742743]

Gregan J, Riedel CG, Pidoux AL, Katou Y, Rumpf C, Schleiffer A, Kearsey SE, Shirahige K, Allshire RC, Nasmyth K. The kinetochore proteins Pcs1 and Mde4 and heterochromatin are required to prevent merotelic orientation. Curr Biol 2007;17:1190–1200. [PubMed: 17627824]

Huang J, Brito IL, Villen J, Gygi SP, Amon A, Moazed D. Inhibition of homologous recombination by a cohesin-associated clamp complex recruited to the rDNA recombination enhancer. Genes Dev 2006;20:2887–2901. [PubMed: 17043313]

Huang J, Moazed D. Association of the RENT complex with nontranscribed and coding regions of rDNA and a regional requirement for the replication fork block protein Fob1 in rDNA silencing. Genes Dev 2003;17:2162–2176. [PubMed: 12923057]

Joglekar AP, Bouck D, Finley K, Liu X, Wan Y, Berman J, He X, Salmon ED, Bloom KS. Molecular architecture of the kinetochore-microtubule attachment site is conserved between point and regional centromeres. J Cell Biol 2008;181:587–594. [PubMed: 18474626]

Joglekar AP, Bouck DC, Molk JN, Bloom KS, Salmon ED. Molecular architecture of a kinetochore-microtubule attachment site. Nat Cell Biol 2006;8:581–585. [PubMed: 16715078]

Johzuka K, Horiuchi T. The cis element and factors required for condensin recruitment to chromosomes. Mol Cell 2009;34:26–35. [PubMed: 19362534]

Kaeberlein M, McVey M, Guarente L. The SIR2/3/4 complex and SIR2 alone promote longevity in Saccharomyces cerevisiae by two different mechanisms. Genes Dev 1999;13:2570–2580. [PubMed: 10521401]

Katis VL, Matos J, Mori S, Shirahige K, Zachariae W, Nasmyth K. Spo13 facilitates monopolin recruitment to kinetochores and regulates maintenance of centromeric cohesion during yeast meiosis. Curr Biol 2004;14:2183–2196. [PubMed: 15620645]

Lee B, Amon A. Meiosis: how to create a specialized cell cycle. Curr Opin Cell Biol 2001;13:770–777. [PubMed: 11698195]

Lee BH, Amon A. Role of Polo-like kinase CDC5 in programming meiosis I chromosome segregation. Science 2003;300:482–486. [PubMed: 12663816]

Li X, Dawe RK. Fused sister kinetochores initiate the reductional division in meiosis I. Nat Cell Biol 2009;11:1103–1108. [PubMed: 19684578]

Lo HC, Wan L, Rosebrock A, Futcher B, Hollingsworth NM. Cdc7-Dbf4 regulates NDT80 transcription as well as reductional segregation during budding yeast meiosis. Mol Biol Cell 2008;19:4956–4967. [PubMed: 18768747]

Longtine MS, McKenzie A 3rd, Demarini DJ, Shah NG, Wach A, Brachat A, Philippsen P, Pringle JR. Additional modules for versatile and economical PCR-based gene deletion and modification in Saccharomyces cerevisiae. Yeast 1998;14:953–961. [PubMed: 9717241]

Marston AL, Amon A. Meiosis: cell-cycle controls shuffle and deal. Nat Rev Mol Cell Biol 2004;5:983–997. [PubMed: 15573136]

Matos J, Lipp JJ, Bogdanova A, Guillot S, Okaz E, Junqueira M, Shevchenko A, Zachariae W. Dbf4-dependent CDC7 kinase links DNA replication to the segregation of homologous chromosomes in meiosis I. Cell 2008;135:662–678. [PubMed: 19013276]

McEwen BF, Heagle AB, Cassels GO, Buttle KF, Rieder CL. Kinetochore fiber maturation in PtK1 cells and its implications for the mechanisms of chromosome congression and anaphase onset. J Cell Biol 1997;137:1567–1580. [PubMed: 9199171]

Mekhail K, Seebacher J, Gygi SP, Moazed D. Role for perinuclear chromosome tethering in maintenance of genome stability. Nature 2008;456:667–670. [PubMed: 18997772]

Monje-Casas F, Prabhu VR, Lee BH, Boselli M, Amon A. Kinetochore orientation during meiosis is controlled by Aurora B and the monopolin complex. Cell 2007;128:477–490. [PubMed: 17289568]

Nasmyth K. Disseminating the genome: joining, resolving, and separating sister chromatids during mitosis and meiosis. Annu Rev Genet 2001;35:673–745. [PubMed: 11700297]

Ohi M, Li Y, Cheng Y, Walz T. Negative Staining and Image Classification - Powerful Tools in Modern Electron Microscopy. Biol Proced Online 2004;6:23–34. [PubMed: 15103397]

Petronczki M, Matos J, Mori S, Gregan J, Bogdanova A, Schwickart M, Mechtler K, Shirahige K, Zachariae W, Nasmyth K. Monopolar attachment of sister kinetochores at meiosis I requires casein kinase 1. Cell 2006;126:1049–1064. [PubMed: 16990132]

Rabitsch KP, Petronczki M, Javerzat JP, Genier S, Chwalla B, Schleiffer A, Tanaka TU, Nasmyth K. Kinetochore recruitment of two nucleolar proteins is required for homolog segregation in meiosis I. Dev Cell 2003;4:535–548. [PubMed: 12689592]

Sinclair DA, Guarente L. Extrachromosomal rDNA circles--a cause of aging in yeast. Cell 1997;91:1033–1042. [PubMed: 9428525]

Smith JS, Boeke JD. An unusual form of transcriptional silencing in yeast ribosomal DNA. Genes Dev 1997;11:241–254. [PubMed: 9009206]

Smith JS, Caputo E, Boeke JD. A genetic screen for ribosomal DNA silencing defects identifies multiple DNA replication and chromatin-modulating factors. Mol Cell Biol 1999;19:3184–3197. [PubMed: 10082585]

Tanaka K, Chang HL, Kagami A, Watanabe Y. CENP-C functions as a scaffold for effectors with essential kinetochore functions in mitosis and meiosis. Dev Cell 2009;17:334–343. [PubMed: 19758558]

Toth A, Rabitsch KP, Galova M, Schleiffer A, Buonomo SB, Nasmyth K. Functional genomics identifies monopolin: a kinetochore protein required for segregation of homologs during meiosis I. Cell 2000;103:1155–1168. [PubMed: 11163190]

Visintin R, Hwang ES, Amon A. Cfi1 prevents premature exit from mitosis by anchoring Cdc14 phosphatase in the nucleolus. Nature 1999;398:818–823. [PubMed: 10235265]

Wei RR, Al-Bassam J, Harrison SC. The Ndc80/HEC1 complex is a contact point for kinetochore-microtubule attachment. Nat Struct Mol Biol 2007;14:54–59. [PubMed: 17195848]

Wei RR, Schnell JR, Larsen NA, Sorger PK, Chou JJ, Harrison SC. Structure of a central component of the yeast kinetochore: the Spc24p/Spc25p globular domain. Structure 2006;14:1003–1009. [PubMed: 16765893]

Wei RR, Sorger PK, Harrison SC. Molecular organization of the Ndc80 complex, an essential kinetochore component. Proc Natl Acad Sci U S A 2005;102:5363–5367. [PubMed: 15809444]

Winey M, Morgan GP, Straight PD, Giddings TH Jr, Mastronarde DN. Three-dimensional ultrastructure of Saccharomyces cerevisiae meiotic spindles. Mol Biol Cell 2005;16:1178–1188. [PubMed: 15635095]

Wong J, Nakajima Y, Westermann S, Shang C, Kang JS, Goodner C, Houshmand P, Fields S, Chan CS, Drubin D, et al. A protein interaction map of the mitotic spindle. Mol Biol Cell 2007;18:3800–3809. [PubMed: 17634282]

Wysocka M, Rytka J, Kurlandzka A. Saccharomyces cerevisiae CSM1 gene encoding a protein influencing chromosome segregation in meiosis I interacts with elements of the DNA replication complex. Exp Cell Res 2004;294:592–602. [PubMed: 15023545]

Yokobayashi S, Watanabe Y. The kinetochore protein Moa1 enables cohesion-mediated monopolar attachment at meiosis I. Cell 2005;123:803–817. [PubMed: 16325576]

Yu H, Braun P, Yildirim MA, Lemmens I, Venkatesan K, Sahalie J, Hirozane-Kishikawa T, Gebreab F, Li N, Simonis N, et al. High-quality binary protein interaction map of the yeast interactome network. Science 2008;322:104–110. [PubMed: 18719252]

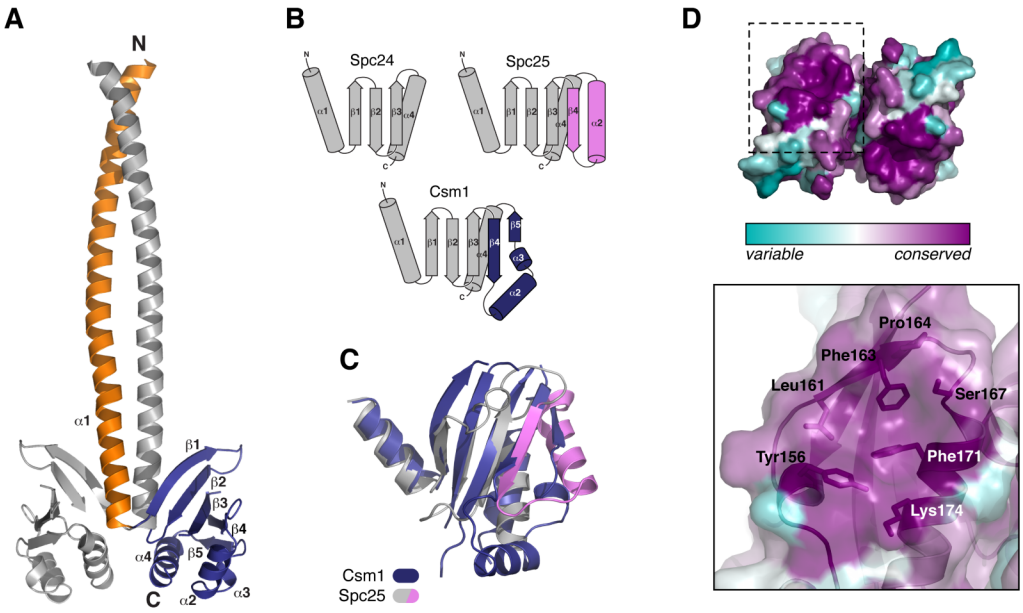

Figure 1. Structure of Csm1

(A) The Csm1 dimer. One chain is shown in orange (N-terminal coiled-coil, residues 3-82) and dark blue (C-terminal globular domain, residues 83-181), the other, in gray. (B) Secondary structure diagrams for Spc24, Spc25, and Csm1, illustrating their common fold (gray) and embellishments in Spc25 (pink) and Csm1 (dark blue). Secondary-structure elements are labeled according to their position in Csm1. (C) Structural overlay of the globular domains of Csm1 (dark blue) and Spc25 (gray/pink, colored as in (B); PDB ID 2FTX (Wei et al., 2006)). The root-mean-squared distance calculated for 57 Cα positions (out of 90) is 1.72 Å. (D) (Upper panel) Bottom view of the Csm1 globular domain dimer, colored according to amino acid conservation among all identifiable Csm1/Pcs1 orthologs in fungi (purple=well conserved, light blue=highly variable; for sequence alignment showing conservation, see Figure S1). (Lower panel) Zoom-in onto the conserved surface boxed in (A), showing the underlying amino acid residues.

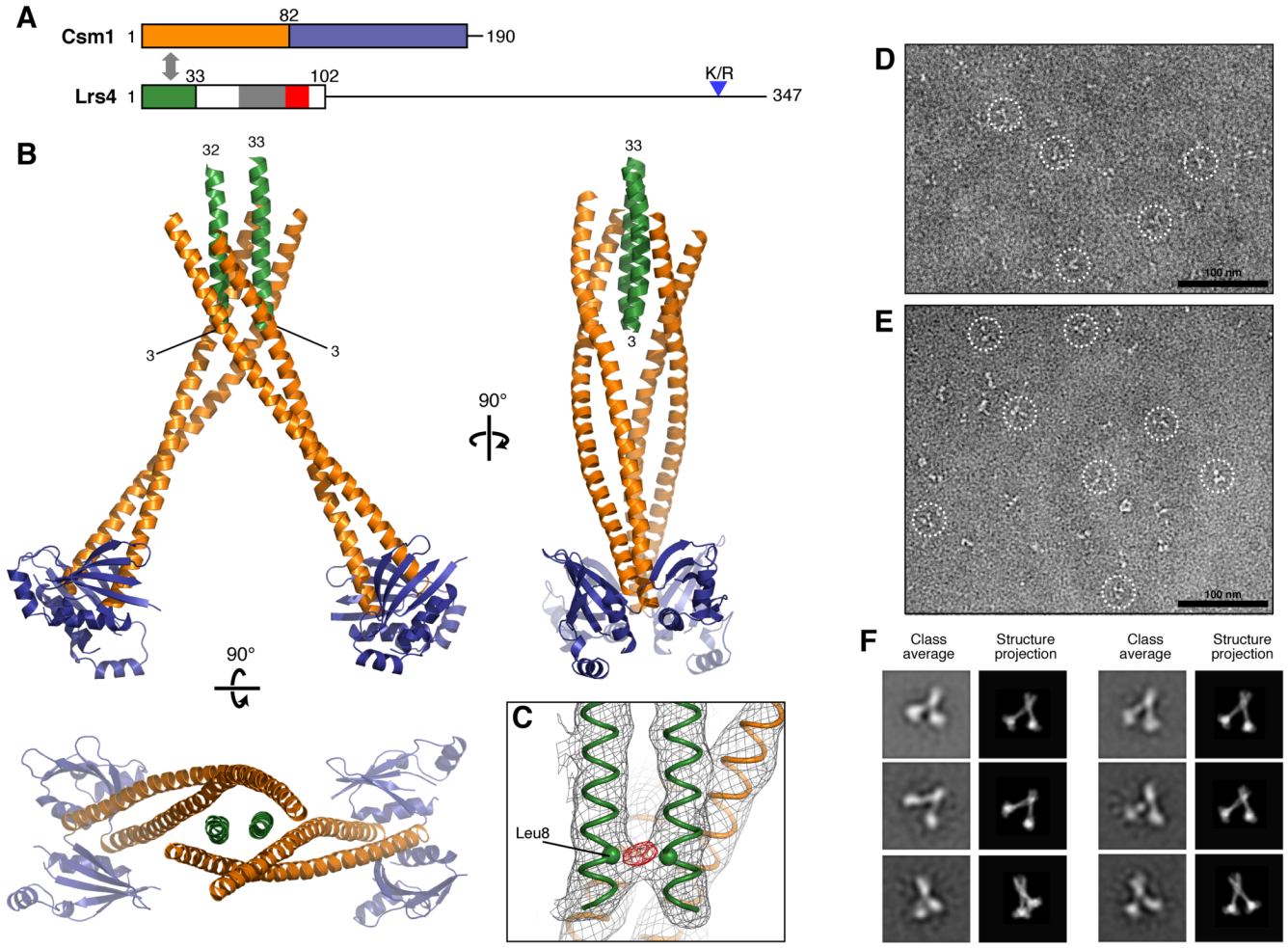

Figure 2. Structure of the Csm1/Lrs4 complex

(A) Diagram of Csm1 and Lrs4 polypeptide chains. Domains of Csm1 are colored as in Figure 1; residues 1-33 of Lrs4 are in green. For Lrs4, predicted coil-coil (residues 54-82) is in gray, and the motif conserved between Lrs4 and *S. pombe* Mde4 (Gregan et al., 2007) in red; a blue arrowhead indicates a lysine/arginine-rich motif (K/R). The gray arrow indicates the interacting regions of the proteins. (B) Orthogonal views of the $(Csm1)_4$:$(Lrs4)_2$ complex, colored as in (A). Residue numbers of the two Lrs4 α-helices are marked. While Lrs4 residues 34-102 were present in the complex as crystallized, they were disordered in the electron density maps. In the crystals, the two Lrs4 α-helices extend into a solvent channel large enough to accommodate these disordered regions (not shown). (C) Electron density surrounding the Lrs4 α-helices. Refined $2F_o$-F_c density (1.2 σ) is in gray, and anomalous difference density from an Lrs4 Leu8→Met selenomethionine (Se-Met) dataset (4.0 σ), is in red. The Cα-atom of Leu8 is shown as a sphere. There is a single strong anomalous difference-density peak directly between the helices, which probably represents the anomalously scattering Se atoms of both Se-Met residues in the Lrs4 dimer. (D) Electron micrograph of negatively stained Csm1/Lrs4 1-102 complex, with representative particles circled. (E) Electron micrograph of the full-length nucleolar Csm1/Lrs4 complex, with representative particles circled. (F) Representative class averages of the full-length Csm1/Lrs4 complex are shown side-by-side with matched resolution-filtered projections of the Csm1/Lrs4 1-102 crystal structure. For more information on the assembly and purification of Csm1/Lrs4 and *S. pombe* Pcs1/Mde4 complexes, see Figure S2.

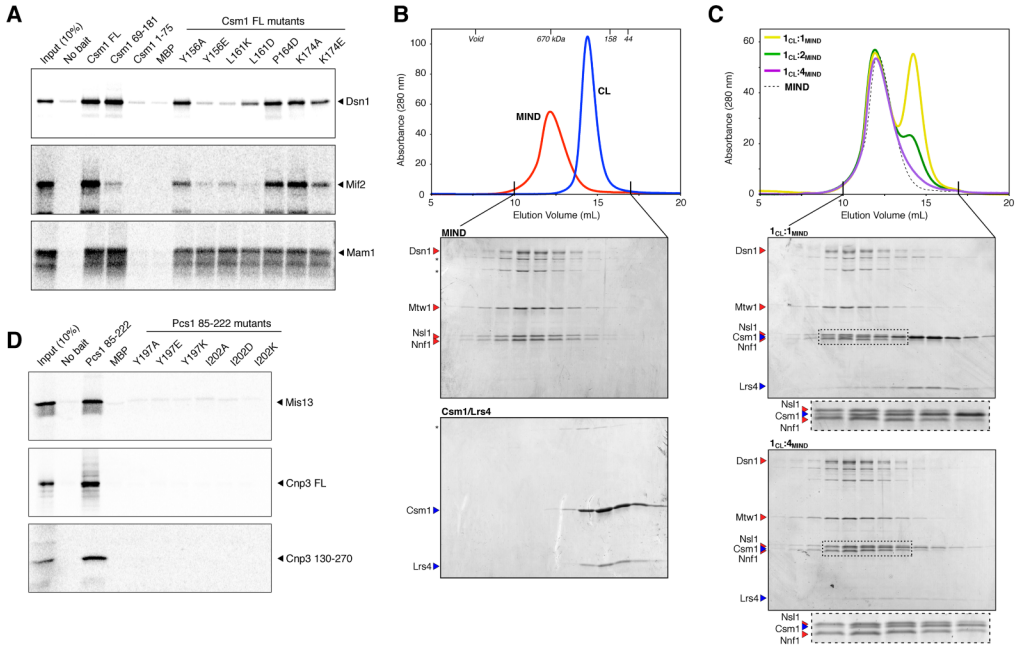

Figure 3. Csm1/Pcs1 binding to the kinetochore subunits Dsn1 and Mif2/CENP-C

(A) *In-vitro* expressed and $^{[35]}$S-labeled Dsn1 (upper panel), Mif2 (middle), and Mam1 (lower) were incubated with purified His_6-tagged Csm1 constructs or point mutants (as indicated), the resulting complexes incubated with Ni^{2+}-affinity resin, and bound proteins analyzed by SDS-PAGE. Point mutations were designed to disrupt the hydrophobic conserved patch identified in Figure 1D. See Figure S3A for a similar analysis using purified S. cerevisiae MIND complex. (B) Superose 6 size exclusion chromatography of 0.2 mg purified MIND (red) and Csm1/Lrs4 (CL; blue) complexes. The migration of molecular weight standards are shown at top. Locations of each band are marked at left of each gel; stars indicate proteolytic products of Dsn1 (MIND; upper panel) or contaminating Hsp70 (Csm1/Lrs4; lower panel). (C) Size exclusion chromatography of MIND/CL mixtures. 1_{CL}:1_{MIND} contained equimolar amounts of the two complete complexes, and 1_{CL}:4_{MIND} contained equimolar amounts of Csm1 (four protomers per CL complex) and the MIND complex. In each mixture, a portion of CL co-migrates with MIND, saturating at one MIND complex per Csm1 protomer (1_{CL}:4_{MIND}). For theoretical curves assuming no interaction, see Figure S3B. CL binding does not significantly alter the elution profile of MIND, potentially because of the extremely extended shape of the MIND complex (see Figure S3C,D). (D) *In-vitro* expressed and $^{[35]}$S-labeled *S. pombe* Mis13 (Dsn1 ortholog; upper panel), Cnp3 (Mif2 ortholog; middle), and Cnp3 residues 130-270 (lower) were incubated with purified His_6-tagged *S. pombe* Pcs1 C-terminal domain (residues 85-222) or point-mutants (as indicated), the resulting complexes incubated with Ni^{2+}-affinity resin, and bound proteins analyzed by SDS-PAGE. All point mutations were in the context of the isolated Pcs1 C-terminal domain, as the full-length protein was poorly behaved in this assay. Y197 and I202 correspond to *S. cerevisiae* Csm1 residues Y156 and L161, respectively (Figure S1).

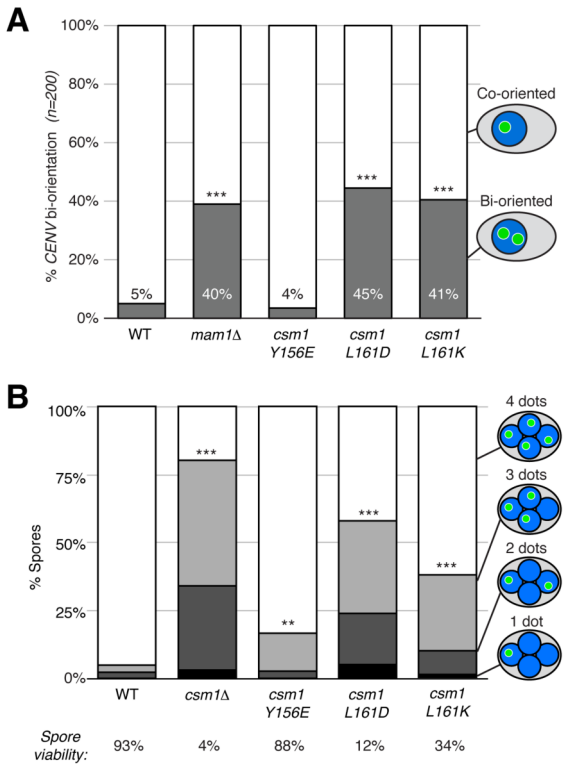

Figure 4. Effects of Csm1 point mutations on *S. cerevisiae* meiotic chromosome segregation

(A) Yeast strains with heterozygous *CENV*-GFP and homozygous monopolin mutations (as noted) were arrested in metaphase I (*pCLB2-CDC20*; (Lee and Amon, 2003)), and scored for sister chromatid bi-orientation (gray) vs. co-orientation (white). Statistical significance values versus wild-type are indicated as stars (3 stars, $P < 0.001$). (B) Yeast strains with *CSM1* mutations or deletion and homozygous *CENV*-GFP were sporulated and examined for chromosome V segregation to spores (2 stars, $P < 0.01$; 3 stars, $P < 0.001$) and for spore viability (data in Table S3).

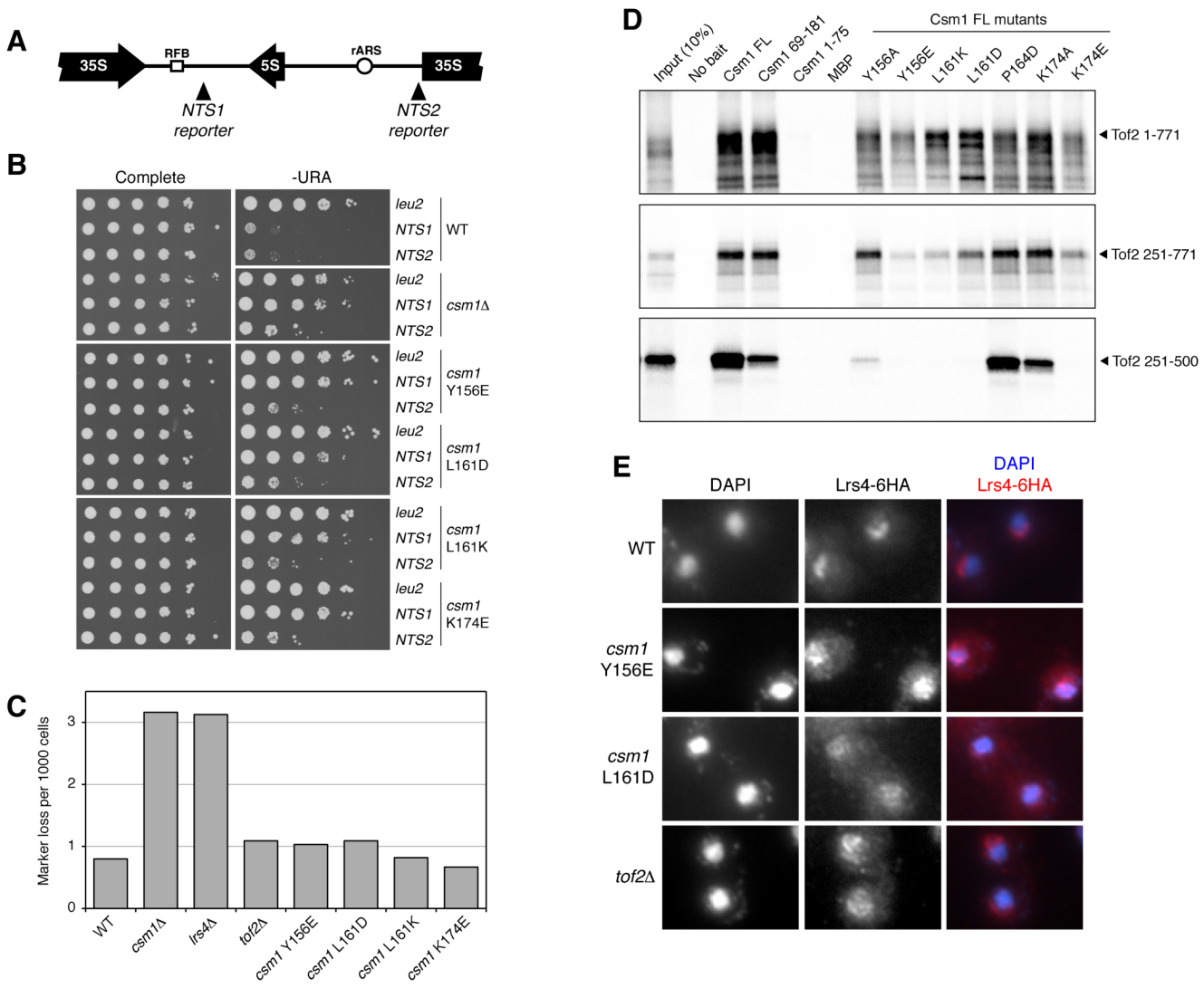

Figure 5. Csm1 binds the rDNA protein Tof2, and Csm1 mutations affect rDNA silencing

(A) Diagram of a single rDNA repeat, with positions of *mURA3* markers inserted into the array at NTS1 and NTS2 noted. 35S and 5S refer to ribosomal genes, RFB; replication fork block sequence, rARS; autonomously replicating sequence. (B) Silencing of an inserted *mURA3* marker (at *leu2*, NTS1, or NTS2 as noted) was assessed by growth on synthetic complete media or media lacking uracil as previously described (Huang et al., 2006). (C) The rate of loss through unequal recombination of an *ADE2* marker inserted into the rDNA array was measured as described previously (Huang et al., 2006; Kaeberlein et al., 1999). For exact values, see Table S4. (D) *In-vitro* expressed and $^{[35]}$S-labeled Tof2 constructs were incubated with His-tagged wild-type and point-mutant Csm1 proteins, and analyzed as in Figure 3. (E) The localization of HA-tagged Lrs4 was examined in interphase, in wild-type and strains with *CSM1* point-mutations or a *TOF2* deletion. The characteristic nucleolar localization of Lrs4 is lost in all of the mutant strains, although some residual nucleolar enrichment is visible in the *TOF2* deletion strain.

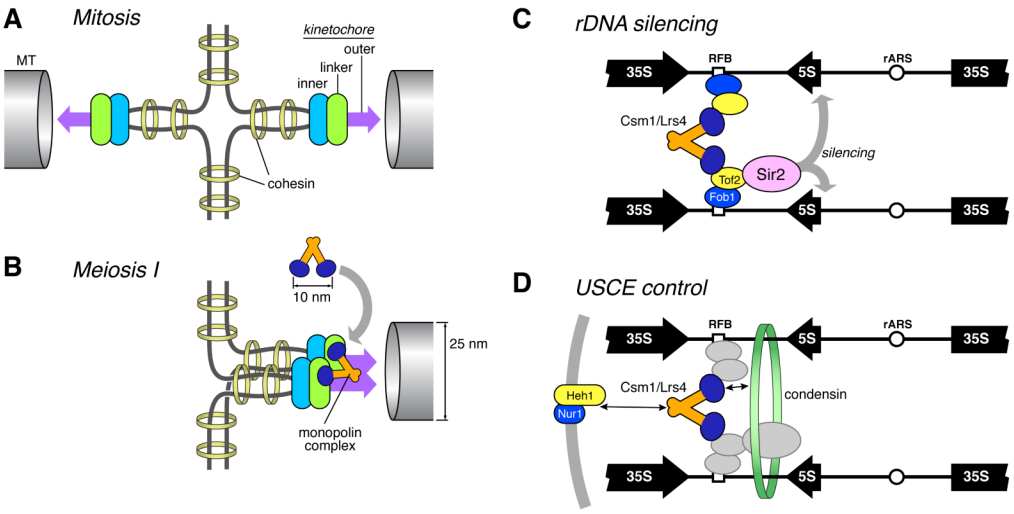

Figure 6. Model for monopolin complex function in *S. cerevisiae*

(A) In *S. cerevisiae* mitosis, sister kinetochores become attached to MTs extending from opposite spindle poles. Sister chromatids (gray lines) are held together by cohesin complexes (yellow rings), and the kinetochores are located at the tips of pericentric chromatin loops. Kinetochores are structurally sub-divided into inner, linker, and outer protein layers (labeled). (B) In meiosis I, sister kinetochores co-orient due to monopolin complex (blue/orange) binding to Mif2 (localized to the inner layer) and Dsn1 (linker layer), effectively fusing their outer kinetochores to form a composite MT-binding site. (C) During interphase, Csm1/Lrs4 binds to rDNA repeats through an rDNA-bound protein complex that includes Fob1, Tof2, and the Sir2-containing RENT complex. Cross-linking of multiple rDNA repeats by Csm1/Lrs4 may aid silencing by localized Sir2. (D) Csm1/Lrs4 likely contributes to the suppression of USCE through interactions with the inner-nuclear membrane proteins Heh1 and Nur1, and condensin complexes. Interactions between this protein network and that controlling rDNA silencing (shown in gray) are currently unknown.

Table 1

Molecular mass determinations from sedimentation equilibrium centrifugation

Protein/Complex	Observed MW (kDa)	Calculated MW (kDa)[1]	Oligomeric state
Csm1 full-length	43.2 +/- 0.9	43.5	2 Csm1
Csm1 1-181	43.4 +/- 1.2	41.2	2 Csm1
Csm1 69-190	29.1 +/- 2.3	28.2	2 Csm1
Pcs1 full-length	53.4 +/- 1.7	51.8	2 Pcs1
Pcs1 85-222	30.1 +/- 2.3	32.2	2 Pcs1
Csm1/Lrs4 full-length	172.3 +/- 4.7	165.6	4 Csm1 + 2 Lrs4
Csm1/Lrs4 1-130	120.4 +/- 3.1	117.6	4 Csm1 + 2 Lrs4
Csm1/Lrs4 1-102	108.5 +/- 3.0	111.0	4 Csm1 + 2 Lrs4
Csm1 1-181/Lrs4 2-30	91.3 +/- 3.1	89.7	4 Csm1 + 2 Lrs4
Pcs1/Mde4 full-length	164.2 +/- 7.8	198.9	4 Pcs1 + 2 Mde4
Pcs1/Mde4 1-231	160.2 +/- 3.6	156.9	4 Pcs1 + 2 Mde4
Pcs1/Mde4 1-125	127.0 +/- 2.7	132.5	4 Pcs1 + 2 Mde4
Pcs1/Mde4 1-77	108.2 +/- 4.1	121.0	4 Pcs1 + 2 Mde4

[1] 'Calculated MW' is the expected molecular mass of a complex with the stoichiometry listed in 'Oligomeric State'.